

Supplementary information

Title: High Spatiotemporal Vessel-Specific Hemodynamic Mapping with Multi-Echo Single-Vessel fMRI

Authors: Yi He, Maosen Wang, and Xin Yu*

Supplementary Figures: 8

Supplementary Tables: 3

Supplementary Movies: 2

Running Title: Multi-Echo Single-Vessel fMRI

Corresponding Author: Xin Yu

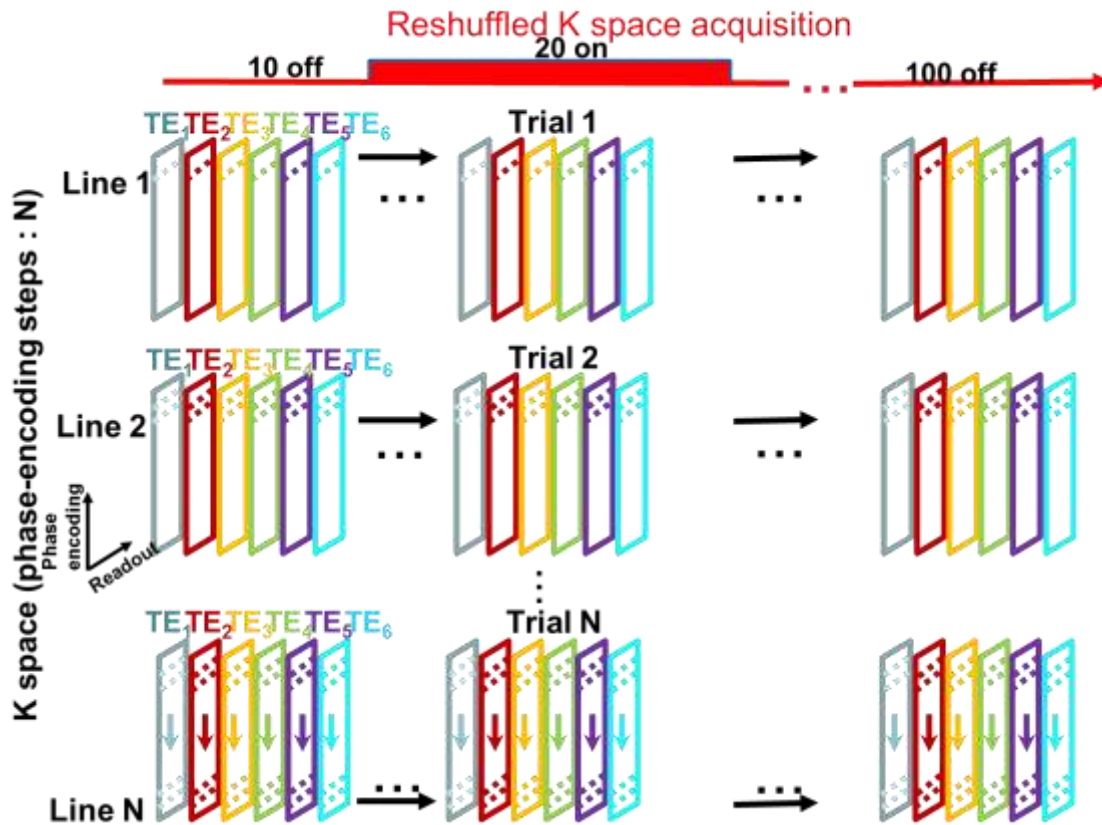
Email: xin.yu@tuebingen.mpg.de, xyu9@mgh.harvard.edu.

Address: Max-Planck-Ring 11, 72076 Tuebingen Germany

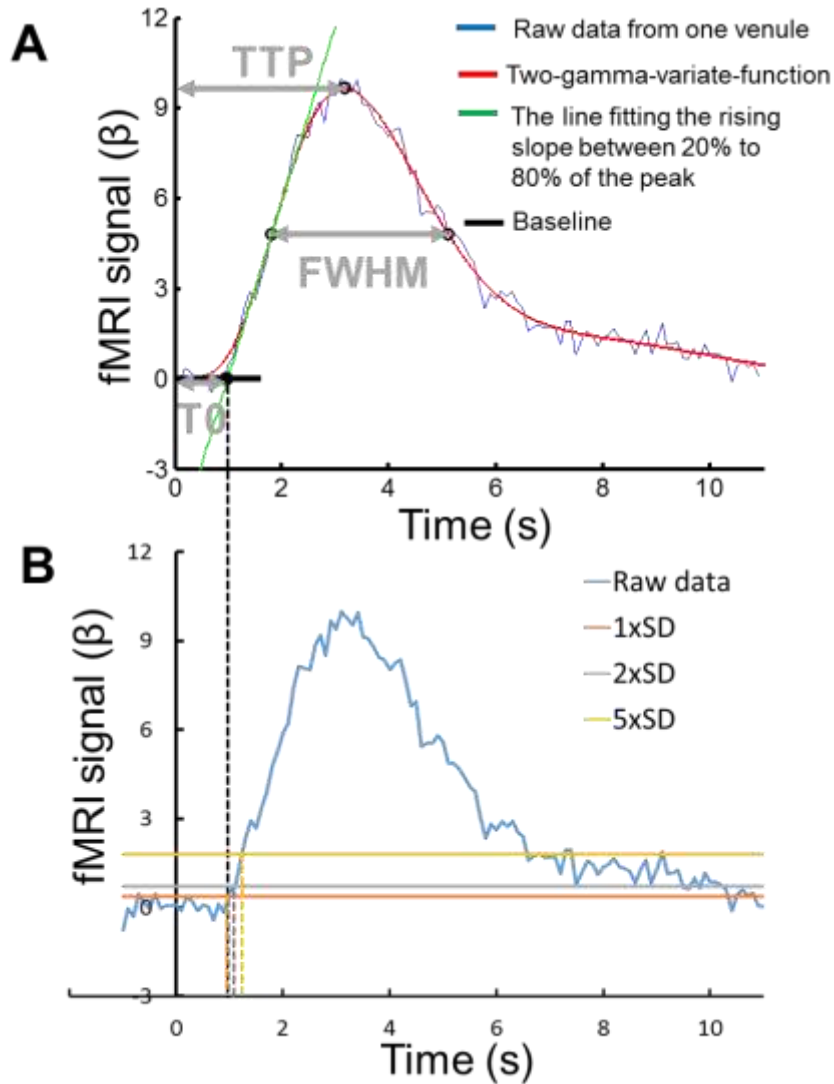
Phone: +49 7071 601-740

Fax: +49 7071 601-701

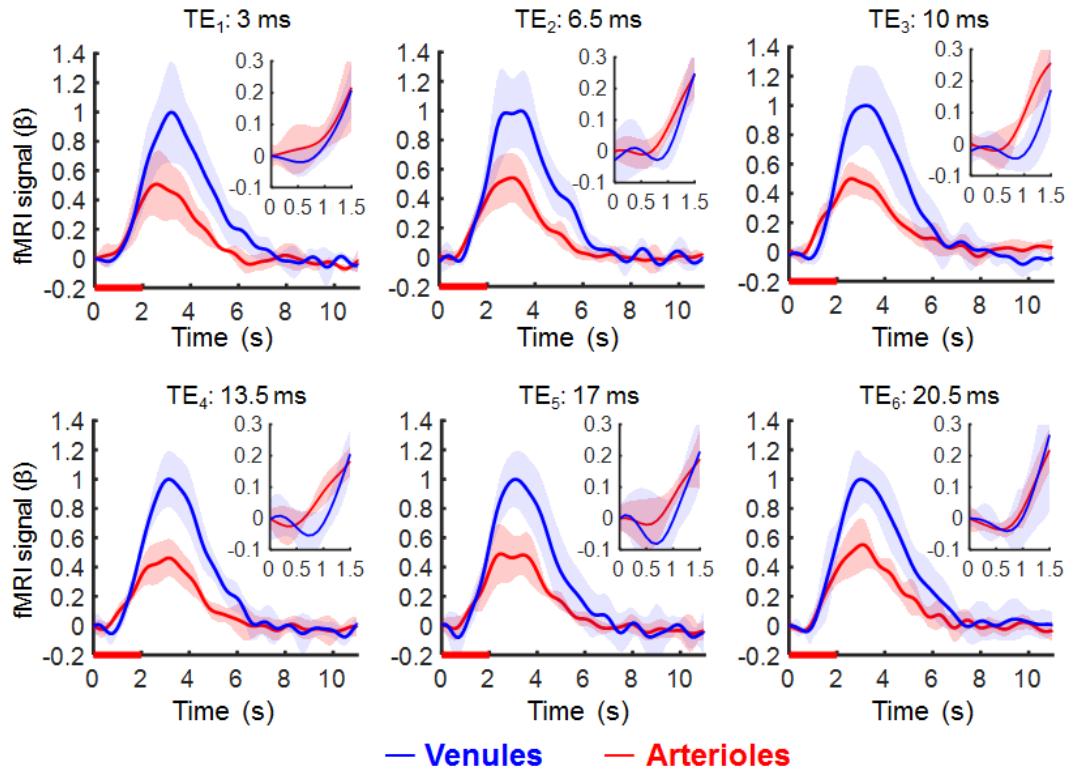
Supplementary Figures (8)



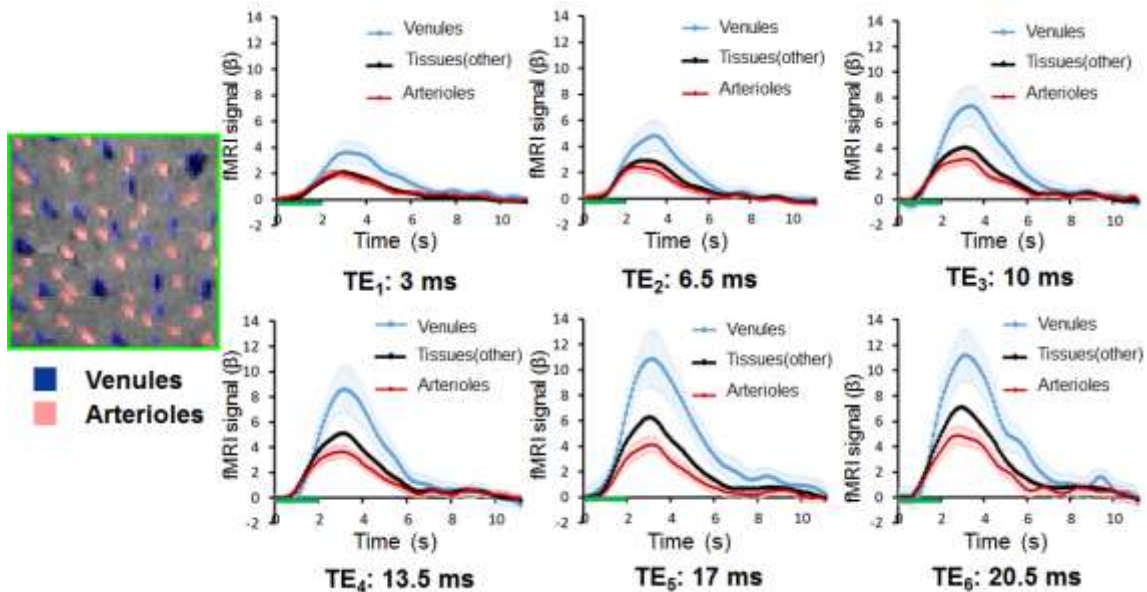
Supplementary Figure 1. K-space Trajectory of Multi-Echo Single-vessel fMRI (MESV-fMRI). The k-space of MELS-fMRI is shown in a block-design paradigm with ten scans off, 20 scans on and 100 scans off (the red line). Each box in different colors represents the k-space of the same slice acquired at different TEs. Within the box, each line indicated a k-space line. One line filled the k-space for each image at each trial consecutively. Then the trials were repeated for the number of phase-encoding steps.



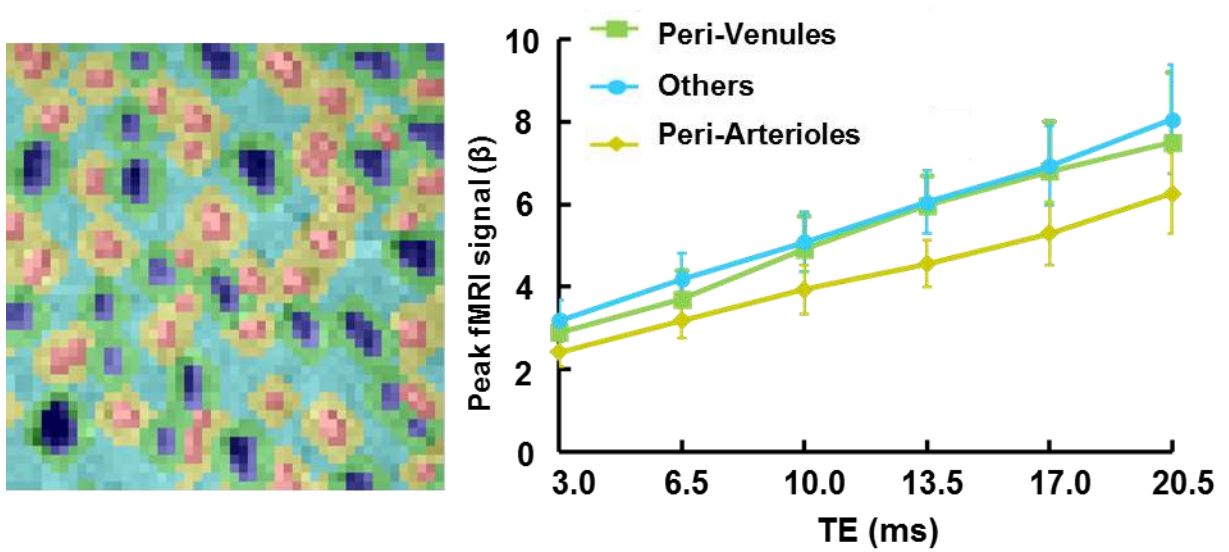
Supplementary Figure 2. The Definition of T0, TTP, FWHM. (A) The raw fMRI signal (blue line) was fitted with the two-gamma-variate function (red line). The green line was the fitting slope of fMRI signal between 20% and 80% to the peak amplitude of two-gamma-variate-function. The T0 was estimated as the intercept with the x-axis. The TTP was estimated by the time from the stimulus onset to the peak amplitude of the two-gamma-variate-function. The FWHM was estimated by the time between two points that are half of the maximum amplitude of the two-gamma-variate-function. **(B)** The onset time T0 defined here is between the first standard deviation (SD) and the second SD from baseline.



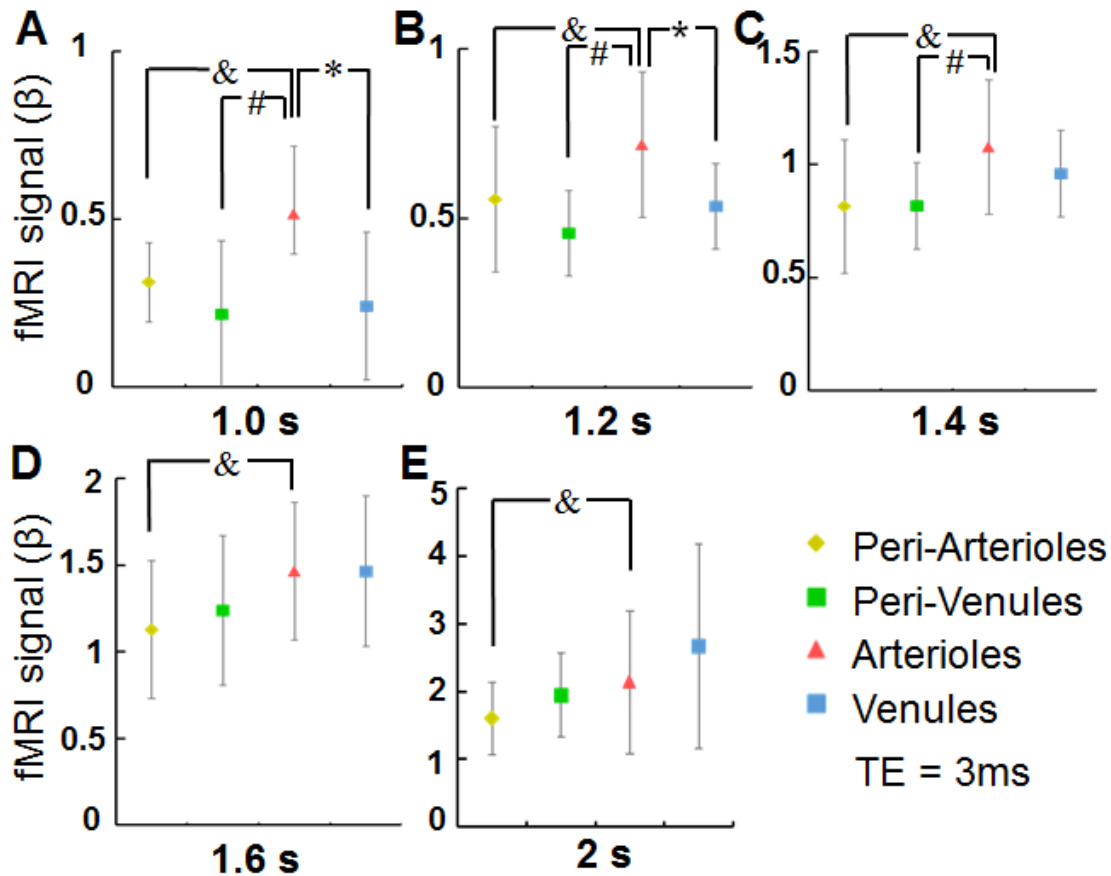
Supplementary Figure 3. The normalized fMRI signal at different TEs from venule and arteriole voxels ($n = 5$ rats, the graphs at different TE, mean \pm SD)



Supplementary Figure 4. The averaged time courses of fMRI signal from venule (blue), arteriole (red) and other non-vessel voxels (black) from one representative rat (mean (95% Confidence Intervals (CI))).

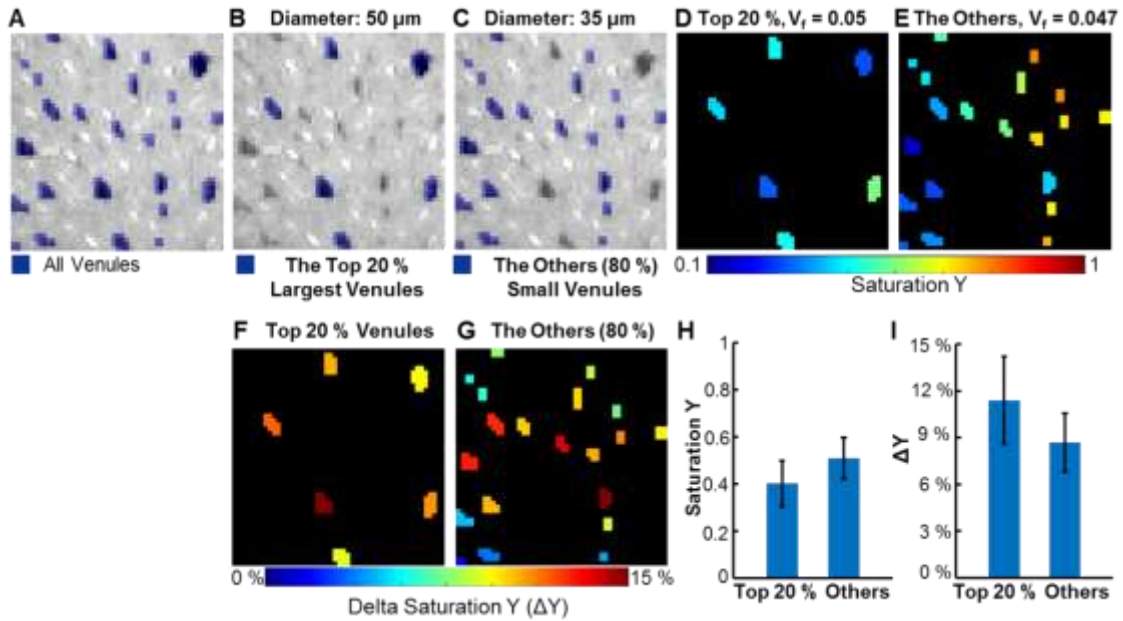


Supplementary Figure 5. The peak amplitudes of fMRI signal from peri-venule (green), peri-arteriole (yellow), and others (cyan) voxels are shown at different TEs ($n = 5$ rats, mean \pm SD). The left panel is an A-V map demo to show the definition of different ROIs.

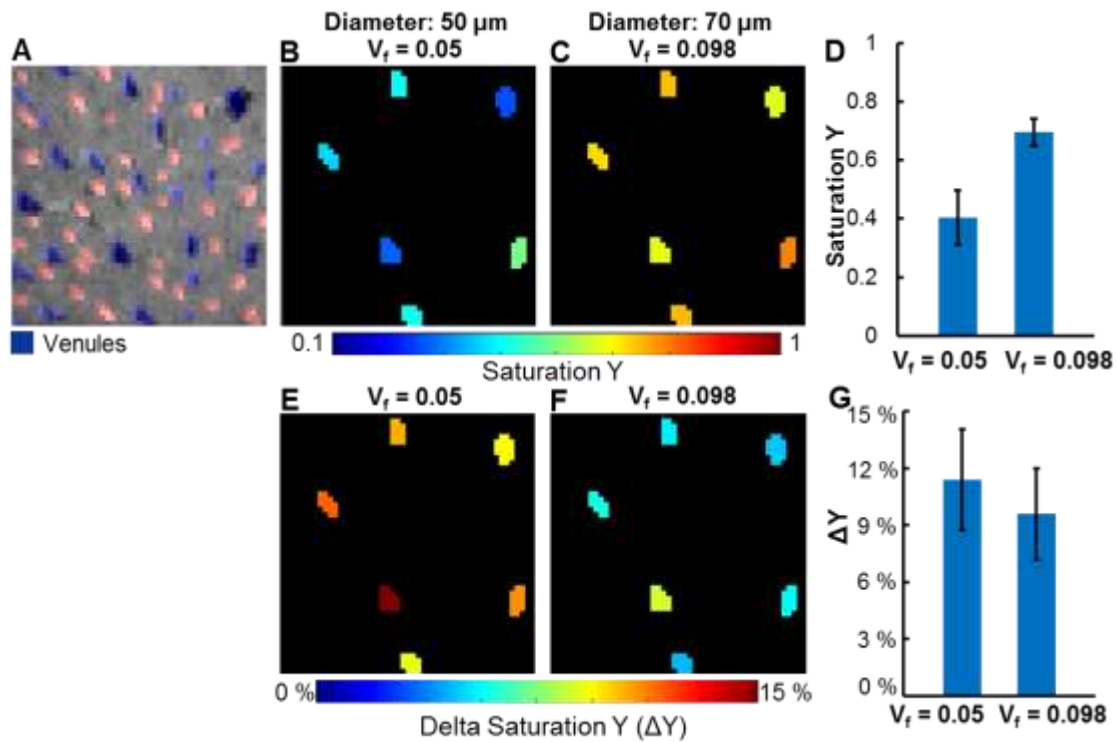


Supplementary Figure 6. Vessel-specific fMRI signal at different time (TE = 3 ms).

The amplitudes (1.0s, 1.2s, 1.4s, 1.6s, 2s after the stimulation onset) of the fMRI signal from arteriole (red), venule (blue), peri-venule (green), and peri-arteriole (yellow) voxels were shown at 3 ms TE (n = 5 rats, mean \pm SD). **(A)** The fMRI signal of arteriole voxels was significantly higher than that of the venule, peri-venule, and peri-arteriole voxels at 1.0s after the stimulation onset. (Paired t-test, n = 5, *, p = 0.009, &, p = 0.04, #, p = 0.037). **(B)** The fMRI signal of arteriole voxels was significantly higher than that of the venule, peri-venule, peri-arteriole voxels at 1.2 s after the stimulation onset. (Paired t-test, n = 5, *, p = 0.025, &, p = 0.047, #, p = 0.034) **(C)** The fMRI signal of arteriole voxels was significantly higher than that of peri-venule and peri-arteriole voxels at 1.4 s after the stimulation onset. (Paired t-test, n = 5, &, p = 0.034, #, p = 0.049) **(D)** The fMRI signal of arteriole voxels was significantly higher than that of peri-arteriole voxels at 1.6 s after the stimulation onset. (Paired t-test, n = 5, &, p = 0.049) **(E)** The fMRI signal of venule voxels was significantly higher than that of arteriole voxels at 2.0 s after the stimulation onset. (Paired t-test, n = 5, &, p = 0.042)



Supplementary Figure 7. The estimated saturation Y maps and saturation changes ΔY maps of the top 20 % largest venules and the others small venules (A) All individual venules (blue) voxels were identified in the A-V map. (B) The top 20 % largest venules voxels were assumed to have 50 μm diameter. (C) The others small venules (80 %) were assumed to have 35 μm diameters. (D-E) The saturation Y maps of the top 20 % largest venules (D, Volume fraction (V_i) = 0.05) and the others 80% small venules (E, V_i = 0.047). (F-G) The saturation changes ΔY maps of the top 20 % largest venules (F) and the others 80 % small venules (G). (H) The mean Y saturation of the top 20 % largest venules ($Y_{V_{20\%}} = 0.403 \pm 0.098$, $N_{\text{venules}_{20\%}} = 6$) and the others 80 % small venules ($Y_{V_{80\%}} = 0.509 \pm 0.088$, $N_{\text{venules}_{80\%}} = 19$, mean (95% CI)). (I) The mean ΔY saturation of the top 20 % largest venules ($\Delta Y_{V_{20\%}} = 11.4 \pm 2.67$ %, $N_{\text{venules}_{20\%}} = 6$, mean (95% CI)) and the others 80 % small venules ($\Delta Y_{V_{80\%}} = 8.71 \pm 1.87$ %, $N_{\text{venules}_{80\%}} = 19$, mean (95% CI))



Supplementary Figure 8. The saturation (Y) and saturation changes (ΔY) of the top 20% largest venules which were assumed to have 50 μm or 70 μm diameter (A) All venules were defined as the blue markers; (B-C) The Y saturation maps of the top 20 % largest venules which were assumed to have 50 μm diameter (B) or 70 μm diameter (C); (D) The mean Y saturation of the top 20 % largest venules which were assumed to have 50 μm diameter ($Y_{V_{20\%}} = 0.403 \pm 0.098$) or 70 μm diameter ($Y_{V_{20\%}} = 0.695 \pm 0.047$, $N_{\text{venules}_{20\%}} = 6$; mean \pm SD) (E-F) The saturation changes ΔY maps of the top 20 % largest venules which were assumed to have 50 μm diameter (E) or 70 μm diameter (F); (G) The mean ΔY saturation of the top 20 % largest venules which were assumed to have 50 μm diameter ($\Delta Y_{V_{20\%}} = 11.4 \pm 2.67$ %) or 70 μm diameter ($\Delta Y_{V_{20\%}} = 9.6 \pm 2.40$ %, $N_{\text{venules}_{20\%}} = 6$, mean \pm SD)

Supplementary Tables (3)

Supplementary Table 1. The volume fraction (V_f) and the calculated saturation (Y) of venules and arterioles with the diameter from 35 μm to 70 μm . ($N_{\text{venules}} = 25$, Venule ROI size: 10.04 ± 1.82 ; $N_{\text{arterioles}} = 35$, Arteriole ROI size: 7.66 ± 0.91 ; mean (95% CI))

Diameter	35 μm		50 μm		70 μm	
	Venules	Arterioles	Venules	Arterioles	Venules	Arterioles
Volume Fraction (V_f)	0.04	0.05	0.07	0.1	0.15	0.2
Saturation (Y)	0.386 ± 0.087	0.741 ± 0.039	0.649 ± 0.050	0.871 ± 0.018	0.836 ± 0.023	0.935 ± 0.010

Supplementary Table 2. The saturation changes (ΔY) of venules and arterioles. ($N_{\text{venules}} = 25$; $N_{\text{arterioles}} = 35$; mean (95% CI); all the venules and arterioles were assumed to have 35 μm , 50 μm and 70 μm , respectively)

Δ Diameter	Diameter V_f	35 μm		50 μm		70 μm	
		0.04	0.05	0.07	0.1	0.15	0.2
Venules:	0 %	$11.14 \pm 1.92 \%$		$6.36 \pm 1.09 \%$		$2.97 \pm 0.52 \%$	
Arterioles:	5 %		$6.53 \pm 0.43 \%$		$3.26 \pm 0.20 \%$		$1.63 \pm 0.12 \%$
	10 %		$9.31 \pm 0.71 \%$		$4.65 \pm 0.37 \%$		$2.33 \pm 0.18 \%$
	15 %		$12.22 \pm 1.25 \%$		$6.11 \pm 0.55 \%$		$3.05 \pm 0.28 \%$

Supplementary Table 3. The V_f , Y and ΔY of the top 20 % largest venules and the others (80 %) small venules. (Top 20 % venules: $N_{\text{venules}_{20\%}} = 6$, the top 20 % largest venules were assumed to have 50 μm diameter; The others 80 % venules: $N_{\text{venules}_{80\%}} = 19$, the others 80 % small venules were assumed to have 35 μm diameters, mean (95 % CI))

Venules	The Top 20 % Largest Venules	The Others (80%) Small Venules
Diameter	50 μm	35 μm
ROI Voxels	15.67 ± 2.167	8.26 ± 1.573
Volume Fraction (V_f)	0.05	0.047
Saturation (Y)	0.403 ± 0.098	0.509 ± 0.088
ΔY	$11.4 \pm 2.80 \%$	$8.71 \pm 1.87 \%$

Supplementary Movies (2)

Supplementary Movie 1. The spatial patterns of the vessel-specific fMRI signal at different TEs. The voxel-wise BOLD fMRI signal was demonstrated from 7x7 voxel matrix covering one individual venule (middle panel: the dark voxel in the green square, in-plane resolution: 50 x 50 μm). The red cursor in the center voxel (100 ms temporal resolution) indicated the fMRI signal changes at 6.5 ms TE (right panel).

Supplementary Movie 2. The T_2^* -based fMRI maps from two representative rats. T_2^* -based fMRI maps (middle panel) were overlapped with the A-V map (left panel). The most active voxels (red color, 100x100 μm) were primarily located at the underlying venule voxels (black dots, right panel).